Title	Theoretical prediction of the linear isomers for rare gas-carbon disulfide complexes : He-CS2, Ne-CS2, and Ar-CS2
Author(s)	Zang, Limin; Dai, Wei; Zheng, Limin; Duan, Chuanxi; Lu, Yunpeng; Yang, Minghui
Citation	Zang, L., Dai, W., Zheng, L., Duan, C., Lu, Y., & Yang, M. (2014). Theoretical prediction of the linear isomers for rare gas-carbon disulfide complexes: He-CS2, Ne-CS2, and Ar-CS2. The Journal of Chemical Physics, 140(11), 114310-.
Date	2014
URL	http://hdl.handle.net/10220/19498
Rights	

Theoretical prediction of the linear isomers for rare gas-carbon disulfide complexes: He-CS2, Ne-CS2, and Ar-CS2

Limin Zang, Wei Dai, Limin Zheng, Chuanxi Duan, Yunpeng Lu, and Minghui Yang

---

Articles you may be interested in

Theoretical prediction of HRgCO + ion (Rg = He , Ne, Ar, Kr, and Xe)
J. Chem. Phys. **129**, 184302 (2008); 10.1063/1.3008057

Accurate intermolecular ground-state potential-energy surfaces of the HCCH–He, Ne, and Ar van der Waals complexes
J. Chem. Phys. **123**, 014309 (2005); 10.1063/1.1947189

Ab initio intermolecular potential-energy surface and microwave spectra for the Ne–OCS complex
J. Chem. Phys. **122**, 234312 (2005); 10.1063/1.1940608

Ground state potential energy curves for He–Kr, Ne–Kr, Ar–Kr, and Kr 2 : Coupled-cluster calculations and comparison with experiment
J. Chem. Phys. **119**, 5487 (2003); 10.1063/1.1600434

Ab initio potential energy surfaces for He–Cl 2 , Ne–Cl 2 , and Ar–Cl 2
J. Chem. Phys. **110**, 7745 (1999); 10.1063/1.478683

Theoretical prediction of the linear isomers for rare gas-carbon disulfide complexes: He-CS$_2$, Ne-CS$_2$, and Ar-CS$_2$

Limin Zang,[1,2] Wei Dai,[1] Limin Zheng,[1,a)] Chuanxi Duan,[2,a)] Yunpeng Lu,[3,a)] and Minghui Yang[1]

[1]*Key Laboratory of Magnetic Resonance in Biological Systems, State Key Laboratory of Magnetic Resonance and Atomic and Molecular Physics, Wuhan Centre for Magnetic Resonance, Wuhan Institute of Physics and Mathematics, Chinese Academy of Sciences, Wuhan 430071, People's Republic of China*
[2]*College of Physical Science and Technology, Central China Normal University, Wuhan 430079, People's Republic of China*
[3]*Division of Chemistry and Biological Chemistry, School of Physical and Mathematical Sciences, Nanyang Technological University, 21 Nanyang Link, Singapore 637371*

Theoretical studies of the potential energy surfaces (PESs) and bound states are performed for rare gas-carbon disulfide complexes, He-CS$_2$, Ne-CS$_2$, and Ar-CS$_2$. Three two-dimensional intermolecular PESs are constructed from *ab initio* data points which are calculated at the CCSD(T) level with aug-cc-pVTZ basis set supplemented with bond functions. We find that the three PESs have very similar features and each PES can be characterized by a global T-shaped minimum, two equivalent local linear minima, and the saddle points between them. The T-shaped isomer is energetically more stable than the linear isomer for each complex. The linear isomers, which have not been observed in experiment so far, are predicted from our PESs and further identified by bound state calculations. Moreover, we assign several intermolecular vibrational states for both the T-shaped and linear isomers of the three complexes via the analysis of wavefunctions. The corresponding vibrational frequencies are calculated from the bound state energies for these assigned states. These frequencies could be helpful for further experimental studies, especially for the linear isomers. We also calculate the rovibrational transition frequencies for the three T-shaped isomers and the pure rotational transition frequencies for the linear isomers, respectively. The accuracy of the PESs is validated by the good agreement between theoretical and experimental results for the rovibrational transition frequencies and spectroscopic parameters. © *2014 AIP Publishing LLC.* [http://dx.doi.org/10.1063/1.4868325]

I. INTRODUCTION

Intermolecular interactions play an important role in many physical, chemical, and biological fields. Van der Waals complex is an ideal model in the research of intermolecular interactions. Such complexes have been extensively studied in both experiment and theory due to the remarkable development in high resolution spectroscopic techniques using supersonic expansion, as well as much availability of high-level *ab initio* calculations in large scale parallel computing environment. These studies have greatly enhanced our understanding on intermoleculaer interactions.

Carbon disulfide (CS$_2$) is a trace gas in the Earth's atmosphere.[1] By interacting with ozone, it could produce both OCS and SO$_2$, occurring in the acid rain chain.[2] It is a nonpolar solvent and has been used in the purification of single-walled carbon nanotubes.[3] At high levels, carbon disulfide may be life-threatening because it affects the nervous system.[4] Species such as CO$_2$, OCS, N$_2$O, and CS$_2$ belong to a class and have similar properties, due to their isovalent electrons. Except for Rg-CS$_2$ (Rg = He, Ne, Ar, Kr, and Xe) complexes, the complexes consisting of such species (CO$_2$,

OCS, N$_2$O) and rare gas atoms have received much attention in both experimental[5–12] and theoretical studies,[13–31] due to their fundamental nature and practical importance. In experiment, the microwave and infrared spectra for these complexes were reported widely[8–12] and showed that each complex has a T-shaped structure. In theoretical calculations, many *ab initio* potential energy surfaces for these complexes have been available in literatures.[16–29] Very similar features are found on their PESs, such as the global "T-shaped" minimum, local linear minima, and saddle points. The intermolecular interactions in these complexes vary systematically with both the polarizability of the rare gas atoms and with the electronic structures of the linear molecules. A local minimum corresponding to a linear structure was found on the PESs for He-CO$_2$ and Ne-CO$_2$ complexes, but such local minima were not found for heavier Rg-CO$_2$ (Rg = Ar, Kr, and Xe) complexes from their *ab initio* PESs. Moreover, the complexes consisting of rare gas atoms and other linear molecules have also been investigated in both theory and experiment, such as Rg-C$_2$H$_2$ (Rg = He, Ne, Ar, Kr, and Xe) complexes.[32–35]

However, Rg-CS$_2$ complexes receive very limited attention, with only an unpublished conference report[36] and relatively a few published results.[37,38] In experiment, Mivehvar and his co-workers observed the first rovibrational spectra for Rg–CS$_2$ (Rg = He, Ne, and Ar) complexes. They measured

a)Electronic addresses: zhenglimin@wipm.ac.cn; cxduan@phy.ccnu.edu.cn; yplu@ntu.edu.sg

the spectra in the CS_2 ν_3 fundamental band for Ar-CS_2, Ne-CS_2 and in both the ν_3 and $\nu_1+\nu_3$ regions for He-CS_2 using a tunable diode laser to probe a pulsed supersonic expansion.[37] They found these complexes have T-shaped structures similar to their CO_2 analogs. In theoretical study, the intermolecular potential energy surfaces of these three Rg-CS_2 (Rg = He, Ne, and Ar) complexes were constructed at the CCSD(T)/aug-cc-pVDZ level with a set of midbond functions ($3s3p2d1f1g$) by Farrokhpour and Tozihi.[38] They found that the PES of each complex could be characterized by a global minimum (T-shaped structure) and two equilibrium linear minima (Linear structures). In order to gain a deeper understanding of the intermolecular interactions for Rg-CS_2 complexes, especially for the stability of the unobserved linear isomers, a new PES with higher accuracy and bound state calculations would be desired for each complex.

In this work, three new high-level *ab initio* PESs are constructed for the Rg–CS_2 (Rg = He, Ne, and Ar) complexes. Bound state calculations are also carried out to study the dynamics for both T-shaped and linear isomers. The accuracy of the PES is assessed by comparison of the rovibrational transition frequencies and spectral parameters for the T-shaped isomers between the theoretical calculation and experimental measurement. Based on the analysis of bound state wavefunctions, some intermolecular vibrational states are assigned unambiguously, which will be useful for the further observation and detailed analysis of experimental spectra, especially for the linear isomers of the Ne-CS_2 and Ar-CS_2 complexes.

This paper is organized as follows: the computational details for the *ab initio* PESs and bound state calculations are described in Sec. II. The results, including the PESs, bound state energy levels, intermolecular vibrational frequencies, and rovibrational transition frequencies are presented in Sec. III. Finally, we conclude in Sec. IV.

II. COMPUTATIONAL DETAILS

A. *Ab initio* calculations of intermolecular potential energy

The CS_2 monomer is assumed to be in its ground vibrational state and is approximated as a linear rigid rotor with C–S bond lengths fixed at its average values of 1.5526 Å.[39] The intermolecular potential energy surface of each Rg-CS_2 complex can be described by two Jacobi coordinates (R, θ) as shown in Fig. 1. R is the distance between the rare gas atom and the center of mass of CS_2. θ denotes the enclosed angle between the R vector and the molecular axis of CS_2. The *ab initio* potential energy grids are chosen as the following: the radial grids include 24 points for He-CS_2, 27 points for Ne-CS_2, and 24 points for Ar-CS_2 complex, respectively, ranging from 1.50 Å to 10.00 Å along the R coordinates, θ varies from 0° to 180° in steps of 15°. Three 2D intermolecular PESs are constructed by executing two one-dimensional interpolations with the Lagrange polynomial formula, respectively. Explicitly, the energy (ε) of given grid point (t) is fitted via the Lagrange interpolation polynomial

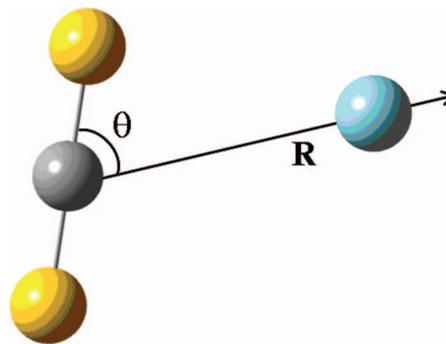FIG. 1. Jacobi coordinates for Rg-CS_2 (Rg = He, Ne, Ar) complex.

formula,

$$\varepsilon(t) = \sum_{i=k}^{k+7} y_i \prod_{j=k, j\neq i}^{k+7} [(t - x_j)/(x_i - x_j)]. \quad (1)$$

Here, x_i and $y_i (i = k,\ldots,k + 7)$ are geometries and *ab initio* intermolecular potential energies, respectively, of the grids. Such interpolation scheme has been employed in our previous studies.[40, 41]

The intermolecular potential energy for each geometry was calculated using the supermolecular method at the level of single and double excitation coupled-cluster method with a noniterative perturbation treatment of triple excitations [CCSD(T)].[42] The aug-cc-pVTZ basis set of Woon and Dunning[43] was employed for all atoms in this study. The bond functions ($3s3p2d1f$) (for $3s$ and $3p$, $\alpha = 0.9, 0.3, 0.1$; for $2d$, $\alpha = 0.6, 0.2$; for f, $\alpha = 0.3$)[44] were also used at the middle point of the intermolecular distance R. The full counterpoise procedure of Boys and Bernardi[45] was employed to correct the basis set superposition error (BSSE). All the calculations were carried out using the Molpro 2010 software package.[46]

B. Bound state calculations

Within the rigid rotor approximation for the linear CS_2 molecular, the Hamiltonian of the Rg-CS_2 complex in Jacobi coordinates can be written as[47–49]

$$\hat{H} = -\frac{1}{2\mu} \frac{\partial^2}{\partial R^2} + \frac{1}{2\mu R^2}(\hat{J} - \hat{j})^2 + B_{CS_2}\hat{j}^2 + V(R,\theta),$$
$$(2)$$

where μ is the reduced mass of the Rg-CS_2 complex, $\hat{J}$ is total angular momentum, and $\hat{j}$ is the angular momentum for CS_2 monomer, and B_{CS_2} is the rotational constant of CS_2 with the value of 0.1091 cm^{-1} in its ground vibrational state and 0.1084 cm^{-1} in its ν_3 excited state,[50] respectively.

The wave function of the system can be expanded as a linear combination of products of the radial and angular basis functions and written as

$$\Psi(R,\theta) = \sum_i \sum_{j,K} c^i_{j,K} \varphi_i(R) Y^{JMK\varepsilon}_j, \quad (3)$$

where $\varphi_i(R)$ are the radial basis function describing the intermolecular stretch and is chosen as sine functions in this work. ε is the index of the space-inverse parity of the system and

$Y_j^{JMK\varepsilon}$ is the total symmetry-adapted angular basis function, which has the following explicit form:

$$Y_j^{JMK\varepsilon} = \frac{1}{\sqrt{2(1+\delta_{K0})}} \times \left[D_{MK}^{*J}(\alpha, \beta, \gamma) Y_{j,K}(\theta, 0) \right.$$
$$\left. + (-1)^\varepsilon D_{M-K}^{*J}(\alpha, \beta, \gamma) Y_{j,-K}(\theta, 0) \right]. \quad (4)$$

The total angular basis function is expressed in the body-fixed frame, where D_{MK}^J is a Wigner rotation matrix to describe the overall rotation of the complex. $Y_{j,K}(\theta, 0)$ is spherical function describing the rotation of CS_2 monomer.

The bound state calculation program was MPI parallelized and the PARPACK software package was applied to solve the eigenvalues and eigenfunctions of the bound states by interfacing our program with a subroutine to calculate $\Phi = \hat{H}\Psi$.[51] In the operation of $\Phi = \hat{H}\Psi$, a method commonly used in the bound state calculations is applied.[52] The central idea of the method is that the kinetic operator matrix is diagonal in finite basis set representation (FBR)[53,54] and the potential energy matrix is diagonal in discrete variable representation (DVR)[55,56] if a convenient basis set is used. In practical calculations, the operation $\Phi = \hat{H}\Psi$ is mainly divided into three steps: (1) at first the trial wavefunction in FBR is multiplied by kinetic operator matrix; (2) in the second step, the trial wavefunction is transformed to DVR and multiplied by the potential energy matrix, and the result is then transformed back to FBR. (3) Summing of the result in the step (1) and (2) and the result is the $\Phi = \hat{H}\Psi$. Such scheme for bound state calculation has been employed in our previous works.[40,57]

Because of the symmetry of the CS_2 molecule, the eigenfunctions of each Rg-CS_2 (Rg = He, Ne, and Ar) complex could be labeled with indexes (ε, j) and are divided into 4 symmetry blocks: $(+1, odd)$, $(+1, even)$, $(-1, odd)$, $(-1, even)$. Each block can be solved separately. The parameters for each complex used in the bound state calculations are listed in Table I. In order to compare our calculations with the experimental results, the rovibrational bound states with a total angular momentum up to $J = 13$ for He-CS_2, $J = 19$ for Ne-CS_2 and $J = 25$ for Ar-CS_2 were calculated for both the vibrational ground and ν_3 excited states of CS_2 molecule, respectively. Although it is only a 2D calculation, the calculations are time-consuming due to the large total angular momentum. Such calculation cost could also be seen from the large number of total basis sets, 31 850 for He-CS_2, 57 600 for Ne-CS_2, and 442 130 for Ar-CS_2 complex, respectively, for the case of J_{tot} = maximum. For potential integrals, two kinds of DVR grids were used for the corresponding basis functions:[52] (1) the equal step grids were used for the intermolecular distance R. The number of the grids equals to the

number of the sine functions in FBR in Table I and (2) the Gauss-Legendre quadrature was used for the angle part. The number of grids ($N_{Gauss-Legendre}$) is listed in Table I. In our calculations, the values of restarts (iterations), k (N_{roots}), and p (N_{shifts}) are varied with J_{tot}, j, and the parity of the system. The largest permitted subspace (m) is the size of the space obtained after expansion. The amount of memory depends on $m = k + p$.[52] Their values for J_{tot} = maximum are listed in Table S1 in the supplementary material.[61]

III. RESULTS AND DISCUSSION

A. *Ab initio* PES

The potential energy surfaces for the three Rg-CS_2 (Rg = He, Ne, and Ar) complexes are presented in Figure 2. It is clear that the three PESs have very similar features and each PES can be characterized by a global minimum, two equivalent local minima, and saddle points between them. The global minimum corresponds to the T-shaped isomer with $\theta = 90.0°$ and the local minima correspond to the linear isomers with $\theta = 0.0°$ or $\theta = 180.0°$. The T-shaped isomers for the three Rg-CS_2 (Rg = He, Ne, and Ar) complexes have been observed in experiment.[37] However, the linear isomers have not been observed experimentally yet.

The geometries and energies of the minima and saddle points on the *ab initio* PESs are listed in Table II. For He-CS_2 complex, the global T-shaped minimum exists at R = 3.407 Å with a depth of -52.953 cm^{-1}. The two equivalent linear local minima are located at R = 5.000 Å with a depth of -30.839 cm^{-1}. The two saddle points connecting the global and the two local minima are located at R = 4.700 Å, $\theta = 47.5°$, or $\theta = 132.5°$, with a height of only 10.915 cm^{-1} relative to the linear local minimum. For Ne-CS_2
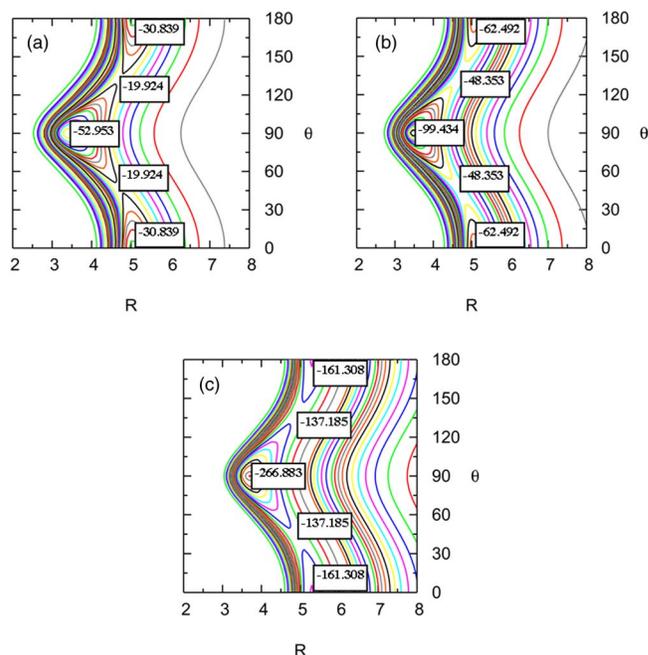
FIG. 2. Contour plots of PES, R in angstrom and θ in degree. (a) He-CS_2 complex; (b) Ne-CS_2 complex; and (c) Ar-CS_2 complex.

TABLE I. Parameters for each complex used in the bound state calculations. The unit of R_{min} and R_{max} is bohr.

	J_{tot}	j_{max}	$N_{Gauss-Legendre}$	N_{sine}	R_{min}	R_{max}
He-CS_2	0–13	70	80	70	4	16
Ne-CS_2	0–19	80	90	80	5	16
Ar-CS_2	0–25	190	200	190	5	16

TABLE II. Important geometries and their corresponding energies on the PES (R in angstrom, angles in degree, and energy in cm^{-1}).

	Global minimum	Local minimum	Saddle point
He-CS_2[a]	(3.407, 90.0, −52.953)	(5.000, 0.0, −30.839)	(4.700, 47.5, −19.924)
		(5.000, 180.0, −30.839)	(4.700, 132.5, −19.924)
Ne-CS_2[a]	(3.470, 90.0, −99.434)	(5.060, 0.0, −62.492)	(4.720, 42.5, −48.353)
		(5.060, 180.0, −62.492)	(4.720, 137.5, −48.353)
Ar-CS_2[a]	(3.700, 90.0, −266.883)	(5.300, 0.0, −161.308)	(4.900, 40.0, −137.185)
		(5.300, 180.0, −161.308)	(4.900, 140.0, −137.185)
He-CS_2[b]	(3.400, 90.0, −58.507)	(5.100, 0.0, −28.422)	(4.675, 41.7, −20.083)
		(5.100, 180.0, −28.422)	(4.675, 138.3, −20.083)
Ne-CS_2[b]	(3.500, 90.0, −103.779)	(5.100, 0.0, −64.387)	(4.598, 41.7, −46.796)
		(5.100, 180.0, −64.387)	(4.598, 138.3, −46.796)
Ar-CS_2[b]	(3.700, 90.0, −272.147)	(5.300, 0.0, −162.520)	(4.866, 44.8, −135.993)
		(5.300, 180.0, −162.520)	(4.866, 135.2, −135.993)

[a]This work.
[b]Taken from Ref. 38.

complex, the PES has a global minimum with a well depth of −99.434 cm^{-1} at R = 3.470 Å. The two equivalent local minima are located at R = 5.060 Å with a depth of −62.492 cm^{-1}. Saddle points connecting the global and two local minima are found at the configuration R = 4.720 Å, θ = 42.5°, or θ = 137.5°, with a barrier of 14.139 cm^{-1} relative to the local minima. For Ar-CS_2 complex, the global minimum has a well depth of −266.883 cm^{-1} at R = 3.700 Å. Local minima are located at R = 5.300 Å with a depth of −161.308 cm^{-1}. The barrier is 24.123 cm^{-1} relative to the local minima with the saddle point at R = 4.900 Å, θ = 40.0°, or θ = 140.0°. We can see that the intermolecular distances become larger and the potential wells become deeper from He-CS_2 to Ar-CS_2 complexes, indicating the intermolecular interactions in these complexes vary systematically with the increasing mass of the rare gas atoms. This is similar to the analogs, such as Rg-X (X = CO_2, N_2O, and OCS) complexes.

To our best knowledge, there is only one theoretical study for Rg-CS_2 complexes so far, which was carried out by Farrokhpour and Tozihi.[38] In their work, they constructed PESs for the same three Rg-CS_2 complexes at CCSD(T)/AVDZ level with basis set extrapolation method. As expected, the two sets of PESs by Farrokhpour and our group have very similar pattern for the three complexes, respectively. From Table II, we can see that the structural parameters agree very well for the three T-shaped isomers in the two works. The corresponding well depths in our PES are slightly shallower than those in Farrokhpour' PESs, with the discrepancy of about 5 cm^{-1} for each complex. However, the locations of the saddle points have obvious differences, especially on the angle part, and the largest discrepancy of that reaches 5.2° in the He-CS_2 complex. Due to the larger basis sets employed in this work, our results would be more reliable.

The important geometries and energies of the Rg-CO_2, Rg-OCS, and Rg-N_2O analogs could be discussed for comparison. The four kinds of complexes have very similar features, such as the global "T-shaped" minimum, local linear minima, and saddle points. The well depth of the global and local minima increases as the mass of the rare gas atom increases in complex. This suggests stronger interactions between the heavier rare gas atoms and the linear molecules. For Rg-OCS[14,18,23,24] and Rg-N_2O[15,17,25–27] complexes, because of the polarity of OCS and N_2O molecules, the global minima deviate from the T-shaped isomer slightly and only a local minimum is found for each complex except for He-OCS, Ne-OCS, and Ne-N_2O complexes. For Rg-CO_2 complexes,[16,19–22] two equivalent local minima (linear isomers) are found for lighter He-CO_2 and Ne-CO_2, but, no local minima is found on PES of the heavier Ar-CO_2, Kr-CO_2, and Xe-CO_2 complexes. Interestingly, although CO_2 and CS_2 are very similar and both are nonpolar, the PESs of Ar-CO_2 and Ar-CS_2 complex have obvious different patterns, especially for the local minima. In detail, there are two local minima on the PES for Ar-CS_2 but no local minimum for Ar-CO_2. This could be explained by the stronger dispersion interaction in linear Ar-CS_2 complexes resulted from the larger polarizability and instantaneous induced dipole moment in CS_2 with more electrons than CO_2 molecule.

B. Intermolecular vibrational states

Bound state calculations have been performed based on our *ab initio* PESs for the three complexes. The intermolecular vibrational excited states could be identified from their wavefunction plots in DVR by counting the number of nodal points or nodal surfaces. In this work, the vibrational states are labeled with two intermolecular vibrational modes ($n_{stretch}$, n_{bent}), where $n_{stretch}$ is the van der Waals stretch vibration and n_{bent} is bent vibration. By analyzing the contour plots, the fundamental vibrational states and several higher excited states are assigned unambiguously for both T-shaped and linear isomers of Ne-CS_2 and Ar-CS_2 complexes. However, for He-CS_2 complex, only the ground states for both the T-shaped and linear isomers are assigned and the excited states could not be assigned because the excited state wavefunctions mix up heavily due to the shallow wells on the PES. The energy levels and vibrational frequencies of the successfully assigned vibrational states for the three complexes are listed in Tables III–V.

TABLE III. The intermolecular vibrational energy levels (in cm^{-1}) and assignments ($n_{stretch}$, n_{bent}) for both T-shaped and linear isomers of the He-CS$_2$ complex.

Assign.	Energy	(ε, j)	No. in block
T-shaped isomer			
(0,0)	-20.776	(1, even)	1
Linear isomer			
(0,0)	-10.017	(1, odd)	1
	-9.920	(1, even)	2

1. He-CS$_2$

For He-CS$_2$ complex, the ground vibrational state of the T-shaped isomer is the 1st root in the (1, even) block with a bound energy of -20.776 cm^{-1}. The corresponding zero point energy is 32.176 cm^{-1}. Because the low barrier (10.915 cm^{-1}) between the global and local minima, the quantum tunneling between the two linear wells occurs with a splitting energy of 0.097 cm^{-1}. Therefore, the two ground vibrational states of the two equivalent linear isomers are not degenerate. The first is the 1st root with the energy of -10.017 cm^{-1} in the (1, odd) block and the zero point energy is 20.822 cm^{-1}. The other is the 2nd root in the (1, even) block with the energy of -9.920 cm^{-1} in the (1, even) block and the zero point energy is 20.919 cm^{-1}. Because the zero point energy (about 20.9 cm^{-1}) of the linear structure is larger than the barrier height (10.915 cm^{-1}) between global and local minima, the linear isomer might not be observed in experiment.

2. Ne-CS$_2$

From Table IV, we can see that the ground state of the T-shaped Ne-CS$_2$ isomer is the 1st root in the (1, even) block with a bound energy of -73.897 cm^{-1}. The corresponding zero point energy is 25.537 cm^{-1}. The intermolecular fundamental vibrational frequencies are 16.131 cm^{-1} for the bend vibrational state and 22.642 cm^{-1} for the stretch vibrational state, respectively.

TABLE IV. The intermolecular vibrational energy levels (in cm^{-1}) and assignments ($n_{stretch}$, n_{bent}) for both T-shaped and linear isomers of the Ne-CS$_2$ complex.

Assign.	Energy	Freq.	(ε, j)	No. in block
T-shaped isomer				
(0,0)	-73.897		(1, even)	1
(0,1)	-57.766	16.131	(1, odd)	1
(1,0)	-51.255	22.642	(1, even)	2
Linear isomer				
(0,0)	-44.035		(1, odd)	2
	-44.035		(1, even)	3
(1,0)	-23.984	20.051	(1, odd)	8
	-23.982	20.053	(1, even)	10
(2,0)	-10.684	33.351	(1, odd)	14
	-10.676	33.359	(1, even)	17

TABLE V. The intermolecular vibrational energy levels (in cm^{-1}) and assignments ($n_{stretch}$, n_{bent}) for both T-shaped and linear isomers of the Ar-CS$_2$ complex.

Assign.	Energy	Freq.	(ε, j)	No. in block
T-shaped isomer				
(0,0)	-233.612		(1, even)	1
(0,1)	-208.695	24.917	(1, odd)	1
(1,0)	-199.607	34.005	(1, even)	2
(0,2)	-184.927	48.685	(1, even)	3
(1,1)	-179.543	54.069	(1, odd)	2
Linear isomer				
(0,0)	-138.553		(1, odd)	6
	-138.553		(1, even)	8
(0,1)	-127.189	11.364	(1, odd)	8
	-127.137	11.416	(1, even)	11
(1,0)	-110.034	28.519	(1, even)	16
	-110.034	28.519	(1, odd)	14
(1,1)	-99.451	39.102	(1, even)	20
	-99.448	39.105	(1, odd)	18
(2,0)	-85.190	53.363	(1, even)	27
	-85.190	53.363	(1, odd)	24
(2,1)	-75.497	63.056	(1, odd)	29
	-75.490	63.063	(1, even)	32

For the linear isomers, the ground vibrational states are doubly degenerate (the 2nd root in the (1, odd) block and the 3rd root in the (1,even) block) with an energy of -44.035 cm^{-1} and a zero point energy of 18.458 cm^{-1}. From Table IV, we can see that the stretch vibrational frequency is 20.051 cm^{-1} (20.053 cm^{-1}). It should be pointed out that the bend vibrational state could not be assigned successfully, because wavefunctions of the bent vibrational state of the linear isomers mix heavily with those of the T-shaped isomer. Besides, two higher excited states (the 14th in the (1, odd) block and 17th in the (1,even) roots) are assigned to the (2, 0) state.

3. Ar-CS$_2$

Due to the deeper well, more vibrational states are assigned successfully for Ar-CS$_2$ complex, as listed in Table V. For the T-shaped isomer, the ground vibrational state has a bound energy of -233.612 cm^{-1} with zero point energy of 33.271 cm^{-1}. From Table V, we can see that four vibrational excited states are assigned unambiguously, they are (0,1), (1,0), (0,2), and (1,1) states. The intermolecular fundamental vibrational frequencies are 24.917 cm^{-1} for the bend vibrational state and 34.005 cm^{-1} for the stretch vibrational state, respectively, which are larger than those of T-shaped Ne-CS$_2$ isomer.

Similar to Ne-CS$_2$ complex, the ground vibrational states of the linear isomers are doubly degenerate (the 6th in the (1, odd) root and the 8th in the (1,even) root) with an energy of -138.553 cm^{-1} and a zero point energy of 22.755 cm^{-1}. Besides, five intermolecular vibrational excited states are assigned totally and listed in Table V. The bend and stretch vibrational frequencies are 11.364 cm^{-1} (11.416 cm^{-1}) and 28.519 cm^{-1} (28.519 cm^{-1}), respectively. The stretch vibrational frequency of the linear Ar-CS$_2$ complex is larger

by 8.5 cm^{-1} than that of linear Ne-CS$_2$ isomer, indicating stronger interaction in linear Ar-CS$_2$ structure than in linear Ne-CS$_2$ structure.

Since there are two equivalent structures for linear Rg-CS$_2$ (Rg = He, Ne, and Ar) complexes, the quantum tunneling effect is an interesting topic to be discussed. As mentioned previously, because of the low barrier (10.915 cm^{-1}) between the global and local minima for He-CS$_2$ complex, the quantum tunneling between the two linear wells occurs with a splitting energy of 0.097 cm^{-1}. For Ne-CS$_2$ and Ar-CS$_2$ complexes, from Tables IV and V, we can see that splitting energies are very small with the largest value of 0.008 cm^{-1} for Ne-CS$_2$ and 0.052 cm^{-1} for Ar-CS$_2$ complex, indicating the quantum tunneling effect is negligible even for the vibrational excited states. Such fact could also be seen directly from the contour plots of wavefunctions in Figs. 3 and 4, where the red and blue lines represent the positive and negative wavefunctions, respectively. We can clearly see that all the wavefunctions of the assigned vibrational states are strongly localized near the local linear minima on PESs, indicating the relative rigidity of the vibrational states and negligible quantum tunneling effect.
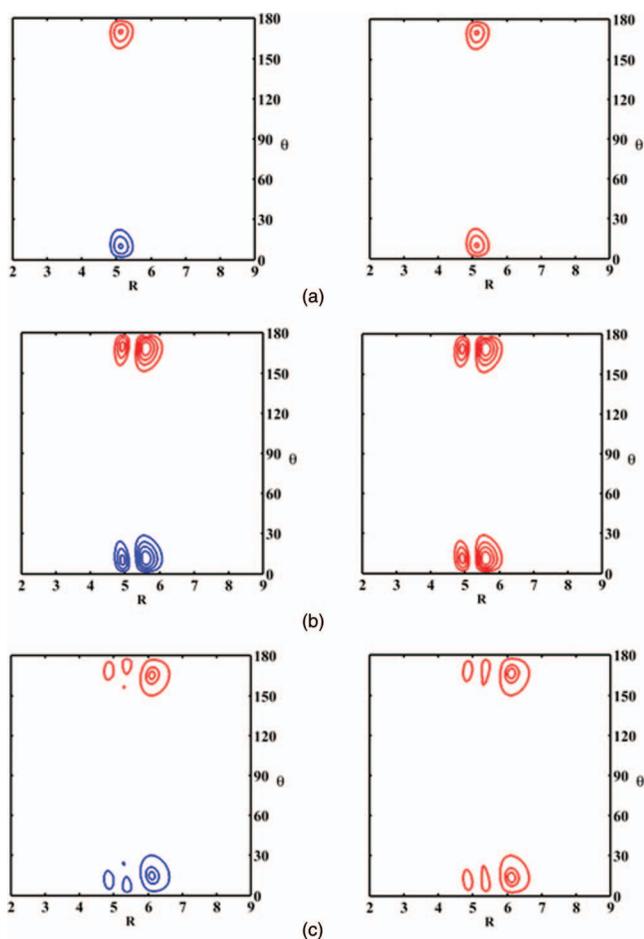

FIG. 3. R-θ contour plots of the wavefunctions for the assigned vibrational states of the linear isomer for Ne-CS$_2$ complexes. The states are assigned by ($n_{stretch}$, n_{bent}). (a) ($n_{stretch}$, n_{bent}) = (0,0); (b) ($n_{stretch}$, n_{bent}) = (1, 0); and (c) ($n_{stretch}$, n_{bent}) = (2,0).
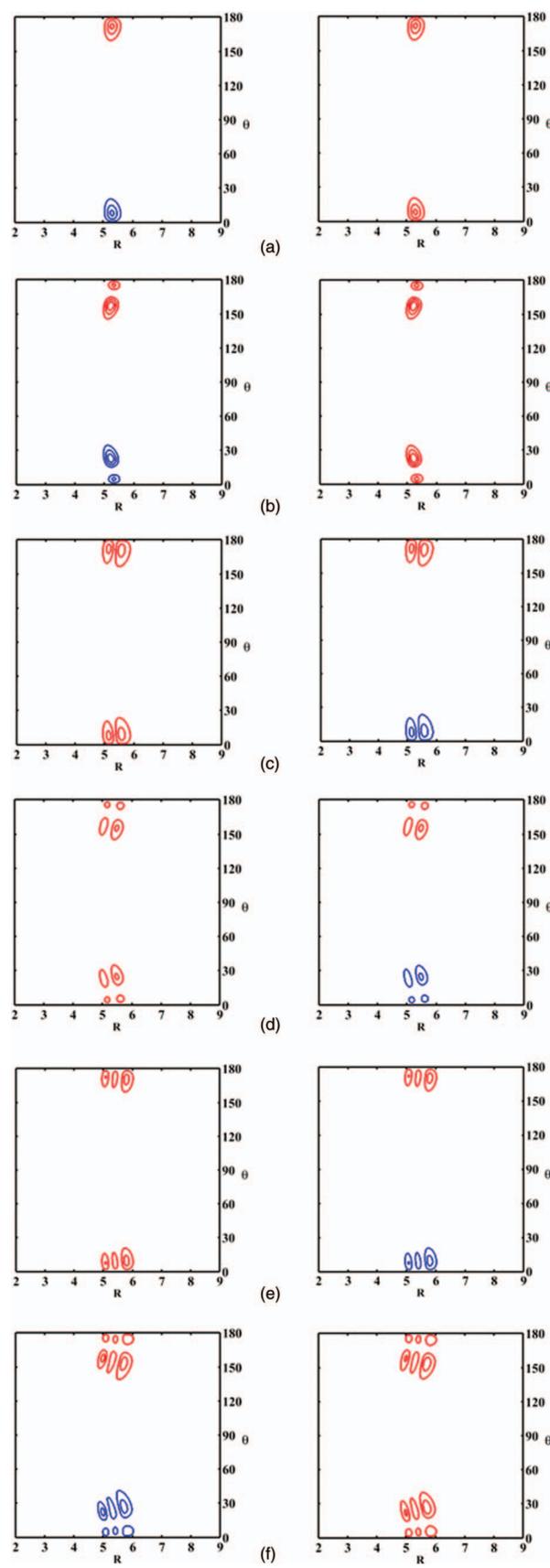

FIG. 4. R-θ contour plots of the wavefunctions for the assigned vibrational states of the linear isomer for Ar-CS$_2$ complexes. The states are assigned by ($n_{stretch}$, n_{bent}). (a) ($n_{stretch}$, n_{bent}) = (0,0); (b) ($n_{stretch}$, n_{bent}) = (0,1); (c) ($n_{stretch}$, n_{bent}) = (1,0); (d) ($n_{stretch}$, n_{bent}) = (1,1); (e) ($n_{stretch}$, n_{bent}) = (2,0); and (f) ($n_{stretch}$, n_{bent}) = (2,1).

TABLE VI. The average structural parameters of the ground vibrational states for both T-shaped and linear isomers (R in angstrom and angles in degree).

| | T-shaped isomer | | Linear isomer |
	Expt.[a]	This work	This work
He-CS$_2$			
$\langle R \rangle$	3.817	3.813	5.262
$\langle \theta \rangle$	79.0	80.6	29.459
Ne-CS$_2$			
$\langle R \rangle$	3.578	3.601	5.139
$\langle \theta \rangle$	86.9	84.0	14.622
Ar-CS$_2$			
$\langle R \rangle$	3.708	3.740	5.305
$\langle \theta \rangle$	86.4	85.6	11.577

[a]Taken from Ref. 37.

C. Average structure parameters

The average structural parameters $\langle R \rangle$ and $\langle \theta \rangle$ for a vibrational state can be determined from the related wavefunctions using the following formulas:[58,59]

$$\left\langle \frac{1}{R^2} \right\rangle \approx \frac{1}{\langle R^2 \rangle} \text{ and } P_2(\cos \langle \theta \rangle) = \langle P_2(\cos \theta) \rangle.$$

P_2 is the second order Legendre function and $\langle P_2(\cos \theta) \rangle$ is the average value of the Legendre function for the state of interest. The calculated structural parameters of the ground states of the Rg-CS$_2$ (Rg = He, Ne, and Ar) complexes for both T-shaped and linear structures are listed in Table VI, as well as the experimental values for the T-shaped isomers. One can see that the calculated average parameters agree well with the experimental values for the T-shaped isomers of the three focused complexes.

It is very interesting to compare the structural parameters between local minima on PES and the vibrationally averaged values. For the T-shaped/linear isomers of the three complexes, the intermolecular distances deviate slightly from the local minima on PES, 0.406 Å/0.262 Å for He-CS$_2$, 0.131 Å/0.079 Å for Ne-CS$_2$, and 0.040 Å/0.005 Å for Ar-CS$_2$ complex, respectively, reflecting the effects of small amplitude motion and zero point energy. For all the isomers, the larger deviations of $\langle \theta \rangle$ from their equilibrium values can be thought

TABLE VII. Calculated pure rotational transition frequencies (in cm^{-1}) of the linear Ne-CS$_2$ and Ar-CS$_2$ isomers.

| | Frequency | |
Transition	Ne-CS$_2$	Ar-CS$_2$
$1 \leftarrow 0$	0.059	0.038
$2 \leftarrow 1$	0.119	0.076
$3 \leftarrow 2$	0.177	0.113
$4 \leftarrow 3$	0.237	0.152
$5 \leftarrow 4$	0.295	0.189

as an effect of vibrational motion of the CS$_2$ monomer in the complex.

D. Rovibrational transition frequencies of the T-shaped isomers

The only available high resolution spectra of the weakly-bound complex Rg–CS$_2$ were recently obtained in the infrared region of the CS$_2$ ν_3 fundamental band, around 1535 cm^{-1}.[37] The observed spectra showed that rare gas-CS$_2$ complexes have T-shaped structures similar to their CO$_2$ analogs. To our best knowledge, the linear isomer has not been successfully observed in experiment so far. As discussed previously, the linear isomers, especially for the Ne-CS$_2$ and Ar-CS$_2$ complexes, might be observed by microwave spectroscopic method. Therefore, we calculated the pure rotation transitional frequencies of the linear Ne-CS$_2$ and Ar-CS$_2$ isomers (See Table VII). These pure rotational energies could be helpful for the observation of linear isomers by microwave spectroscopy.

In the next section, we will limit our discussion to the rovibrational spectra for the T-shaped isomers of the three Rg-CS$_2$ complexes. Since the available infrared spectra of Rg–CS$_2$ complexes involve the CS$_2$ ν_3 asymmetric stretch mode, rotational energy levels of the complex with CS$_2$ in both the ground state and the ν_3 state were calculated. The calculated rotational energy levels and the assignments of the three T-shaped isomers are available in Tables S2–S4 in the supplementary material.[61]

In order to obtain the theoretical values for these transitions from the calculated energy levels, we used the

TABLE VIII. Comparison of the spectroscopic parameters (in cm^{-1}) and the inertial defects (in amu Å^2) for the T-shaped He-CS$_2$ complex.

| | $\nu_3 = 0$ | | $\nu_3 = 1$ | |
Parameter	Expt.[a]	Calc.	Expt.[a]	Calc.
A	0.32156(47)	0.31573(87)	0.32076(47)	0.31593(89)
B	0.111322(21)	0.111376(47)	0.110604(18)	0.110646(47)
C	0.080321(23)	0.079818(38)	0.079845(19)	0.079460(35)
Δ_j	$6.70(110) \times 10^{-7}$	$1.02(53) \times 10^{-6}$	$6.70(11) \times 10^{-7}$	$1.06(41) \times 10^{-6}$
Δ_k	$3.14(77) \times 10^{-4}$	$4.37(118) \times 10^{-4}$	$3.34(73) \times 10^{-4}$	$4.57(116) \times 10^{-4}$
Δ_{jk}	$1.077(33) \times 10^{-4}$	$1.078(55) \times 10^{-4}$	$1.078(30) \times 10^{-4}$	$1.072(50) \times 10^{-4}$
δ_k	$6.34(67) \times 10^{-5}$	$7.61(136) \times 10^{-5}$	$6.44(60) \times 10^{-5}$	$7.40(116) \times 10^{-5}$
Inertial defect	6.06	6.45	6.16	6.43

[a]Taken from Ref. 37.

TABLE IX. Comparison of the spectroscopic parameters (in cm^{-1}) and the inertial defects (in amu Å^2) for the T-shaped Ne-CS$_2$ complex.

Parameter	$\nu_3 = 0$		$\nu_3 = 1$	
	Expt.[a]	Calc.	Expt.[a]	Calc.
A	0.1104648(177)	0.1104513(249)	0.1097503(153)	0.1097436(216)
B	0.0844484(127)	0.0829502(176)	0.0843890(120)	0.0829616(166)
C	0.0472047(107)	0.0467536(150)	0.0470475(103)	0.0466289(145)
Δ_j	$1.198(87) \times 10^{-6}$	$1.757(119) \times 10^{-6}$	$1.374(73) \times 10^{-6}$	$1.781(101) \times 10^{-6}$
Δ_k	$-1.104(43) \times 10^{-5}$	$-9.18(62) \times 10^{-6}$	$-1.051(33) \times 10^{-5}$	$-9.00(47) \times 10^{-6}$
Δ_{jk}	$9.85(26) \times 10^{-6}$	$7.64(35) \times 10^{-6}$	$9.243(223) \times 10^{-6}$	$7.521(305) \times 10^{-6}$
δ_j	$6.54(37) \times 10^{-7}$	$7.76(49) \times 10^{-7}$	$7.06(32) \times 10^{-7}$	$7.78(44) \times 10^{-7}$
δ_k	$6.755(200) \times 10^{-6}$	$6.194(286) \times 10^{-6}$	$6.655(157) \times 10^{-6}$	$6.240(228) \times 10^{-6}$
Inertial defect	4.89	4.71	4.95	4.72

[a]Taken from Ref. 37.

expression

$$v = E_0 - E(\nu_3 = 1) - E(\nu_3 = 0),$$

where E$_0$ is a vibrational origin. However, our intermolecular potential was calculated for fixed CS$_2$ geometries, and so does not vary with CS$_2$ vibrational state. The CS$_2$ vibrational dependence of the Rg–CS$_2$ energy levels was partly included by varying the CS$_2$ rotational constant. This approximation has proven to be rather effective for rotation spacings,[49] but it cannot accurately represent the possible vibrational shift of the complex origin, E$_0$, relative to the free monomer origin. In the present case, we obtain a value for E$_0$ by simply comparing a well-defined observed transition with the theoretical result and use this for the remaining theoretical transition frequencies. Specifically, the well-defined observed transition is selected to be 1535.534 cm^{-1} (101-000) for He-CS$_2$, 1535.553 cm^{-1} (111-000) for Ne-CS$_2$, and 1535.449 cm^{-1} (111-202) for Ar-CS$_2$, respectively.

Because the amount of data is too large, the theoretical transition frequencies and their deviations from experimental values are given in Tables S5–S7 in the supplementary material for the three complexes,[56,61] respectively. The RMSD between the experimental and calculated values is only 0.008 cm^{-1} for He-CS$_2$, 0.010 cm^{-1} for Ne-CS$_2$, and 0.012 cm^{-1} for Ar-CS$_2$ complex, respectively. The good

agreement between the theory and experiment confirms the high accuracy of our *ab initio* PESs.

In order to compare the spectroscopic parameters with experimental values directly, the theoretical rotational energy levels are fitted with the same Hamiltonian used in the experiment, a Watson asymmetric rotor expression employing the A-type reduction in the *Ir* representation,[60]

$$H = \frac{1}{2}(B + C)J^2 + \left[A - \frac{1}{2}(B + C)\right]J_a^2$$
$$+ \frac{1}{2}(B - C)(J_b^2 - J_c^2) - \Delta_J J^4 - \Delta_{JK} J_a^2 J^2$$
$$- \Delta_K J_a^4 - 2\delta_J J^2(J_b - J_c) - \delta_k$$
$$\times \left[J_a^2(J_b^2 - J_c^2) + (J_b^2 - J_c^2)J_a^2\right].$$

The fitted parameters show excellent agreement with the corresponding experimental values[37] (see Tables VIII–X). The inertial defects are also listed in Table VIII–X for complexes both in CS$_2$ ground state and ν_3 excited state. We can see that the inertial defects also show good overall agreement with the corresponding experimental values, with the maximum discrepancy of 0.43 amu Å^2 for the Ar-CS$_2$ complex in CS$_2$ ν_3 excited state. The discrepancy can be explained by the fact that the rotational constants are fitted by all the rotational

TABLE X. Comparison of the spectroscopic parameters (in cm^{-1}) and the inertial defects (in amu Å^2) for the T-shaped Ar-CS$_2$ complex.

Parameter	$\nu_3 = 0$		$\nu_3 = 1$	
	Expt.[a]	Calc.	Expt.[a]	Calc.
A	0.1099010(107)	0.1102150(125)	0.1091882(110)	0.1093048(114)
B	0.0470672(50)	0.0464187(49)	0.0470456(53)	0.0463043(46)
C	0.0327650(43)	0.0324928(49)	0.0326910(40)	0.0323679(49)
Δ_j	$1.891(11) \times 10^{-7}$	$7.792(114) \times 10^{-7}$	$1.828(117) \times 10^{-7}$	$0.6594(105) \times 10^{-6}$
Δ_k	$-1.23(37) \times 10^{-6}$	$-3.70(42) \times 10^{-6}$	$-1.36(30) \times 10^{-6}$	$-2.83(33) \times 10^{-6}$
Δ_{jk}	$1.705(60) \times 10^{-6}$	$2.090(73) \times 10^{-6}$	$1.708(53) \times 10^{-6}$	$1.743(64) \times 10^{-6}$
δ_j	$4.937(400) \times 10^{-8}$	$4.937(400) \times 10^{-8}$	$4.937(434) \times 10^{-8}$	$4.937(434) \times 10^{-8}$
δ_k	$1.418(80) \times 10^{-6}$	$1.418(80) \times 10^{-6}$	$1.321(67) \times 10^{-6}$	$2.874(24) \times 10^{-6}$
Inertial defect	2.95	2.69	2.95	2.52

[a]Taken from Ref. 37.

energy levels calculated in this work but fitted by only the resolved transitions in experiment.

IV. CONCLUSIONS

In this paper, theoretical studies of the potential energy surface and bound states were performed for the Rg-CS_2 (Rg = He, Ne, and Ar) van der Waals complex. Three two-dimensional intermolecular potential energy surfaces were constructed at the CCSD(T) level with aug-cc-pVTZ basis set supplemented with bond functions. We find that the three PESs have very similar features and each PES can be characterized by a global T-shaped minimum, two equivalent local linear minima and saddle points between them. For each complex, the T-shaped isomer is energetically more stable than the linear isomer and the T-shaped isomer has been observed in experiment. However, the linear isomers have not been observed experimentally yet.

Intermolecular vibrational states for both T-shaped and linear isomers are assigned from the analysis of their wavefunctions. For He-CS_2 complex, because of the low well and the heavily mixing of wavefunctions, only the vibrational ground states are assigned for both T-shaped and linear isomers. For Ne-CS_2 and Ar-CS_2 complexes, due to their deep wells and high barriers, several higher vibrational excited states are also assigned successfully besides their fundamental vibrational states for T-shaped and linear isomers. Accordingly, the corresponding vibrational frequencies are obtained from the bound state energies of these assigned states. These results could be helpful to further spectroscopic studies in experiment, especially for the linear isomers.

Quantum tunneling effect is also discussed for the three complexes. We find quantum tunneling effects for the ground state between the two linear isomers of He-CS_2 complex, with a splitting energy of 0.097 cm^{-1}. However, quantum tunneling effects are negligible in the ground states of the linear isomers and the ground states are doubly degenerate for both Ne-CS_2 and Ar-CS_2 complexes. This could be explained by the deep well and high barrier between two local linear isomers.

The calculated rovibrational frequencies are compared with the experimental frequencies for the T-shaped isomers of three complexes, respectively. The RMSD between the experimental and calculated values is 0.008 cm^{-1} for He-CS_2, 0.010 cm^{-1} for Ne-CS_2, and 0.012 cm^{-1} for Ar-CS_2 complex, respectively. The good agreement between the theory and experiment confirms the high accuracy of our *ab initio* PESs.

ACKNOWLEDGMENTS

[1] B. M. R. Jones, R. A. Cox, and S. A. Penkett, J. Atmos. Chem. **1**, 65 (1983).
[2] M. A. K. Khalil and R. A. Rasmussen, Atmos. Environ. **18**, 1805 (1984).
[3] T.-J. Park, S. Banerjee, T. Hemraj-Benny, and S. S. Wong, J. Mater. Chem. **16**, 141 (2006).
[4] P. J. Klemmer and A. A. Harris, Am. J. Kidney Dis. **36**, 626 (2000).
[5] G. T. Fraser, A. S. Pine, and R. D. Suenram, J. Chem. Phys. **88**, 6157 (1988).
[6] F. J. Lovas and R. D. Suenram, J. Chem. Phys. **87**, 2010 (1987).
[7] W. A. Herrebout, H.-B. Qian, H. Yamaguchi, and B. J. Howard, J. Mol. Spectrosc. **189**, 235 (1998).
[8] R. Zheng, Y. Zhu, S. Li, and C. X. Duan, Mol. Phys. **109**, 823 (2011).
[9] J. M. Sperhac, M. J. Weida, and D. J. Nesbitt, J. Chem. Phys. **104**, 2202 (1996).
[10] D. S. Zhu, R. B. Wang, R. Zheng, G. M. Huang, and C. X. Duan, J. Mol. Spectrosc. **253**, 88 (2009).
[11] R. Zheng, D. S. Zhu, Y. Zhu, and C. X. Duan, J. Mol. Spectrosc. **263**, 174 (2010).
[12] J. Tang and A. R. W. McKellar, J. Chem. Phys. **115**, 3053 (2001).
[13] G. Maroulis and A. Haskopoulos, Chem. Phys. Lett. **349**, 335 (2001).
[14] E. Feng, C. Y. Sun, C. H. Yu, X. Shao, and W. Y. Huang, J. Chem. Phys. **135**, 124301 (2011).
[15] H. Zhu, D. Q. Xie, and G. Yan, J. Comput. Chem. **24**, 1839 (2003).
[16] M. Chen and H. Zhu, J. Theor. Comput. Chem. **11**, 537 (2012).
[17] Y. Z. Zhou, D. Q. Xie, and D. H. Zhang, J. Chem. Phys. **124**, 144317 (2006).
[18] H. Zhu, Y. Z. Zhou, and D. Q. Xie, J. Chem. Phys. **122**, 234312 (2005).
[19] Y. L. Cui, H. Ran, and D. Q. Xie, J. Chem. Phys. **130**, 224311 (2009).
[20] R. Chen, H. Zhu, and D. Q. Xie, Chem. Phys. Lett. **511**, 229 (2011).
[21] R. Chen, E. Jiao, H. Zhu, and D. Q. Xie, J. Chem. Phys. **133**, 104302 (2010).
[22] H. Ran and D. Q. Xie, J. Chem. Phys. **128**, 124323 (2008).
[23] H. Zhu, Y. Guo, Y. Xue, and D. Q. Xie, J. Comput. Chem. **27**, 1045 (2006).
[24] H. Li and Y.-T. Ma, J. Chem. Phys. **137**, 234310 (2012).
[25] H. Zhu, D. Q. Xie, and G. S. Yan, Chem. Phys. Lett. **351**, 149 (2002).
[26] R. Chen and H. Zhu, J. Theor. Comput. Chem. **7**, 1093 (2008).
[27] J. X. Chen, H. Zhu, D. Q. Xie, and G. S. Yan, Acta Chim. Sinica **62**, 5 (2004); available at http://sioc-journal.cn/Jwk_hxxb/EN/Y2004/V62/I1/5.
[28] L. C. Wang, D. Q. Xie, R. J. Le Roy, and P.-N. Roy, J. Chem. Phys. **137**, 104311 (2012).
[29] H. Li, R. J. Le Roy, Phys. Chem. Chem. Phys. **10**, 4128 (2008).
[30] X. G. Wang, T. Carrington, Jr., Can. J. Chem. **88**, 779 (2010).
[31] X. G. Wang, T. Carrington, Jr., J. Tang, and A. R. W. McKellar, J. Chem. Phys. **123**, 034301 (2005).
[32] C. Lauzin, L. H. Coudert, M. Herman, and J. Liévin, J. Phys. Chem. A **117**, 13767 (2013).
[33] C. Lauzin, E. Cauët, J. Demaison, M. Herman, H. Stoll, and J. Liévin, Mol. Phys. **110**, 2751 (2012).
[34] B. Fernández, C. Henriksen, and D. Farrelly, Mol. Phys. **111**, 1173 (2013).
[35] C. R. Munteanu and B. Fernández, J. Chem. Phys. **123**, 014309 (2005).
[36] M. A. Walsh, A. Lewin, Y. D. Juang, J. Cruzan, C. H. Hwang, and T. R. Dyke, 47th Ohio State University International Symposium on Molecular Spectroscopy, Paper TG-09, 15–19 June, 1992; see http://hdl.handle.net/1811/12898.
[37] F. Mivehvar, C. Lauzin, A. R. W. McKellar, and N. Moazzen-Ahmadi, J. Mol. Spectrosc. **281**, 24 (2012).
[38] H. Farrokhpour and M. Tozihi, Mol. Phys. **111**, 779 (2013).
[39] D. R. Lide, *CRC Handbook of Chemistry and Physics*, 88th ed. (CRC Press, Boca Raton, FL, 2008).
[40] L. M. Zheng, Y. P. Lu, S.-Y. Lee, H. Fu, and M. H. Yang, J. Chem. Phys. **134**, 054311 (2011).
[41] L. M. Zheng, S.-Y. Lee, Y. P. Lu, and M. H. Yang, J. Chem. Phys. **138**, 044302 (2013).
[42] C. Hampel, K. Peterson, and H. J. Werner, Chem. Phys. Lett. **190**, 1 (1992).
[43] D. E. Woon and T. H. Dunning, J. Chem. Phys. **98**, 1358 (1993).
[44] T. B. Pedersen, B. Fernandez, H. Koch, and J. Makarewicz, J. Chem. Phys. **115**, 8431 (2001).
[45] S. F. Boys and F. Bernardi, Mol. Phys. **19**, 553 (1970).
[46] H. J. Werner, P. J. Knowles, G. Knizia, F. R. Manby, M. Schütz *et al.*, MOLPRO, version 2010.1, a package of *ab initio* programs, 2010, see http://www.molpro.net.
[47] S. Miller and J. Tennyson, J. Mol. Spectrosc. **128**, 530 (1988).
[48] S. Y. Lin and H. Guo, J. Chem. Phys. **117**, 5183 (2002).
[49] J. Tennyson and B. T. Sutcliffe, Mol. Phys. **51**, 887 (1984).
[50] J. S. Wells, M. Schneider, and A. G. Maki, J. Mol. Spectrosc. **132**, 422 (1988).
[51] R. Lehoucq, D. C. Sorensen, and C. Yang, *ARPACK User's Guide: Solution of Large-Scale Eigenvalue Problems with Implicitly Restarted*

Arnoldi Methods (SIAM, Philadelphia, PA, 1998), see http://www.caam.rice.edu/software/ARPACK.

[52] R. B. Lehoucq, S. K. Gray, D. H. Zhang, and J. C. Light, Comput. Phys. Commun. **109**, 15 (1998).

[53] G. C. Corey, J. W. Tromp, and D. Lemoine, in *Numerical Grid Methods and Their Applications to Schrödinger Equation*, NATO ASI Series C Vol. 412, edited by C. Cerjan (Kluwer Academic, New York, 1993), p. 1.

[54] M. J. Bramley, J. W. Tromp, T. Carrington, Jr., and G. C. Corey, J. Chem. Phys. **100**, 6175 (1994).

[55] D. O. Harris and G. G. Engerholm, J. Chem. Phys. **43**, 1515 (1965).

[56] J. C. Light and T. Carrington, Jr., Adv. Chem. Phys. **114**, 263 (2000).

[57] L. Wang, M. H. Yang, A. R. W. Mckellar, and D. H. Zhang, Phys. Chem. Chem. Phys. **9**, 131 (2007).

[58] J. Zhu, Y.-P. Lu, X.-R. Chen, and Y. Cheng, Eur. Phys. J. D **33**, 43 (2005).

[59] H. Ran, Y. Z. Zhou, and D. Q. Xie, J. Chem. Phys. **126**, 204304 (2007).

[60] M. J. Weida, J. M. Sperhac, D. J. Nesbitt, and J. M. Hutson, J. Chem. Phys. **101**, 8351 (1994).

[61] See supplementary material at http://dx.doi.org/10.1063/1.4868325 for the parameters in bound state calculations in PARPACK, rotational energy levels and transition frequencies of the T-shaped isomers.